JCTC Journal of Chemical Theory and Computation

Article

pubs.acs.org/JCTC

Adaptive Resolution Simulation (AdResS): A Smooth Thermodynamic and Structural Transition from Atomistic to Coarse Grained Resolution and Vice Versa in a Grand Canonical Fashion

Han Wang, Christof Schütte, and Luigi Delle Site*

Institute for Mathematics, Freie Universität Berlin, Berlin, Germany

ABSTRACT: The AdResS method in molecular dynamics (MD) allows, in a grand canonical (GC) fashion, to change on-the-fly the number of degrees of freedom of a system, allowing to pass from atomistic (AT) to coarse-grained (CG) resolution and vice versa as a function of the position of the molecule in the simulation box. The coupling of resolutions is made in a thermodynamically consistent way, though in the current formulation, in the region where the molecule changes resolution, neither thermodynamic nor structural properties can be preserved. Here we propose an extension of the method where basic thermodynamic and structural properties can be systematically controlled also in the transition region; this assures a very smooth change from one molecular representation to the other. Moreover, we provide a rigorous argument which shows that if in the region where the molecules change resolution the radial distribution function (RDF) is the same as in the AT and CG region, then the AT region is, from the statistical point of view, equivalent to a subsystem embedded in a larger full AT system, at least up to a second order approximation.

1. INTRODUCTION

Bridging scales in condensed matter, material science or chemical physics is equivalent to describing the connection between local processes and the emerging global behavior of the system. In this context, molecular simulation has the final aim of understanding the molecular origin of large scale properties, and this can be viewed as a sort of process of zooming in (to the details) and zooming out (to the large scale properties) as pictorially illustrated in the example of Figure 1. Standard molecular simulation techniques do not allow the zooming process in a concurrent fashion, that is considering different resolutions at the same time. Rather, the zooming process is done in a sequential hierarchical way in a bottom-up or top-down fashion.[1] Ideally, a computational magnifying glass as in Figure 1 should be designed as an adaptive resolution approach. This means that it should (1) change molecular resolution in a region of space keeping the rest of the system at lower resolution; (2) allow for the free exchange of molecules between the different regions, so that natural particle number fluctuations are not arbitrarily suppressed; and (3) points 1 and 2 must occur under conditions of thermodynamic equilibrium which are the same as if the whole system was described at higher resolution. This implies that (at least) the temperature and particle density are the same in the AT and CG region, and are the same for a full AT simulation of reference.[1] The computational advantages are obvious: simpler models requires less computational energies and thus can be more efficient. However, the real advantage of a method of this kind is in its conceptual consequences: it can in principle identify the essential degrees of freedom (DOFs) of a system and thus avoid producing an excess of details which may overshadow the essential physics or chemistry of the system. A method with the characteristics outlined above is the adaptive resolution simulation (AdResS) scheme[2,3] whose basic aspects are reported in the next section. Methods similar to AdResS or dealing with mixed atomistic-coarse grained resolution have also been presented in the literature in the past few years; for a general overview see refs 4−9. In this work we propose an extension of the AdResS method which allows an even smoother transition from one resolution to the other. On the basis of such an extension we then give theoretical arguments which make the general theoretical framework more solid.

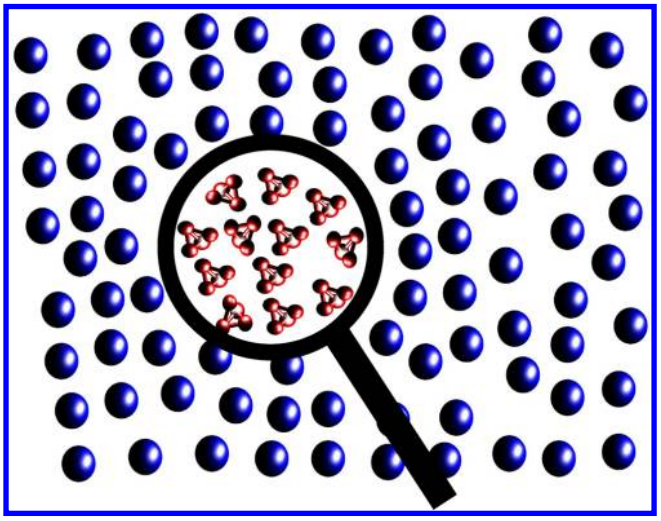

Figure 1. Magnifying glass illustrates the idea of zooming in to the AT scale to understand the molecular origin of the statistical properties of a liquid which at larger scale can be viewed as a collection of spheres, a resolution sufficient to represent the large scale behavior.

Received: April 30, 2012
Published: June 27, 2012

2. ADRESS: BASIC ASPECTS

The AdResS method allows an on-the-fly interchange between the AT and CG description (and vice versa) of the molecules according to their position in space. The two resolutions are coupled across scales by dividing the system into three parts (see also Figure.2): (a) a high resolution region (AT) with atomistic details; (b) a low resolution region (CG) with a simple-sphere representation of molecules; and (c) a transition region (Δ) within which molecules continuously adapt resolution through a space dependent interpolation of the high and low resolution intermolecular forces

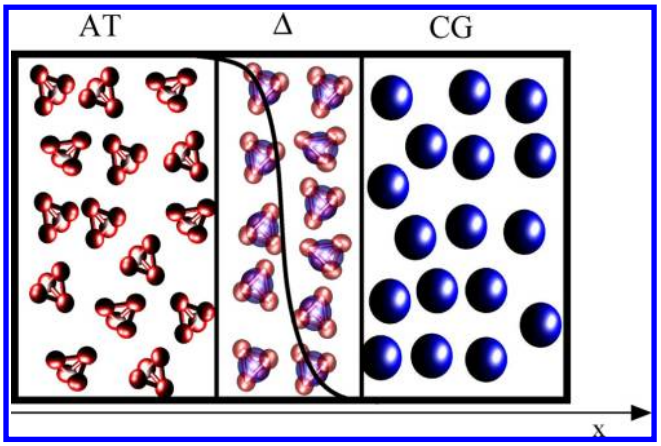

Figure 2. Schematic representation of the adaptive simulation box. Molecules moving from the atomistic region (AT) region slowly lose their resolution passing through continuous level of hybrid resolution in the transition region, Δ, and then becoming spheres in the coarse-grained region (CG) (and vice versa). The example shown here consists of a liquid of tetrahedral molecules, that is, the toy model used for developing the AdResS method.[2] The region Δ in realistic applications should be much smaller than the AT and CG region; here, Δ is enlarged in order to make pictorially clear the hybrid resolution and the shape of $w(x)$.

$$\mathbf{F}_{\alpha\beta} = w(x_\alpha)w(x_\beta)\mathbf{F}^{\mathrm{AT}}_{\alpha\beta} + [1 - w(x_\alpha)w(x_\beta)]\mathbf{F}^{\mathrm{CG}}_{\alpha\beta} \quad (1)$$

where α and β label two molecules, $\mathbf{F}^{\mathrm{AT}}_{\alpha\beta}$ is the force derived from the AT potential and $\mathbf{F}^{\mathrm{CG}}_{\alpha\beta}$ is the force derived from the CG potential acting on the centers of mass (COMs), $w(x)$ is a function with value zero in the CG region, one in the AT and smooth and monotonic in the transition region Δ. The standard form of $w(x)$ currently used in the AdResS scheme is

$$w(x) = \begin{cases} 1 & x < d_{\mathrm{AT}} \\ \cos^2\left[\dfrac{\pi}{2(d_\Delta)}(x - d_{\mathrm{AT}})\right] & d_{\mathrm{AT}} < x < d_{\mathrm{AT}} + d_\Delta \\ 0 & d_{\mathrm{AT}} + d_\Delta < x \end{cases} \quad (2)$$

where d_{AT} and d_Δ are the size of the atomistic and hybrid region, respectively, and x is the x-coordinate of the COM of a molecule measured along the x-axis as defined in Figure 2. (In the water simulation presented in Section 7, d_{AT} = 0.5 nm and d_Δ = 2.75 nm.) Notice that throughout the paper we assume a fixed volume and the application of periodic boundary conditions. Therefore $w(x)$ is also fixed and periodic. The CG potential is derived from a reference full AT simulation and is such that it reproduces structural or thermodynamic properties of the reference full AT system; later we will discuss the coarse-graining procedure in more detail. The way the force of eq 1 acts between the molecules is illustrated in Figure 3. The basic idea behind this approach is that the smooth force interpolation minimally disturbs the dynamics in either of the participating regions when a molecule changes side.

It is obvious that the approach is non-Hamiltonian; that is, it does not exist a potential from which the force of eq 1 can be derived. In practice, the energy drift of the system is taken care by a Langevin thermostat with globally uniform parameters. This has been shown both analytically[10] and with detailed computer experiments.[9] The question which naturally emerges at this point is how to ensure thermodynamic equilibrium if we

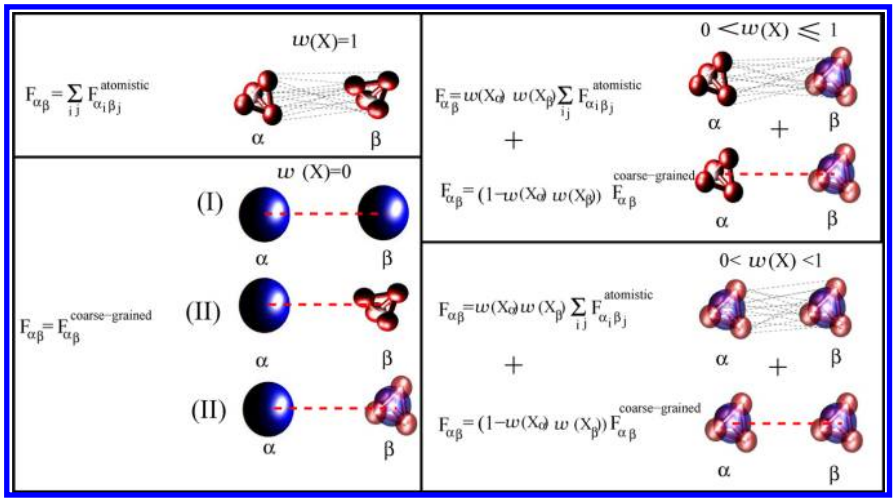

Figure 3. How $\mathbf{F}_{\alpha,\beta}$ acts between the molecules. Two AT molecules (i.e., $w(x)$ = 1) interact as standard AT molecules, that is, each atom i of α with each atom j of β. Two GC molecules, $w(x)$ = 0, interact via the COM (no atomistic DOFs present). Each molecule interacting with a CG molecule must interact only via the COM because the CG molecule does not have other DOFs. Technically the force acting on the COM for a hybrid or AT molecule is then redistributed on the atoms according to the mass of each. For the case of the tetrahedral molecule shown here, it means that the force is redistributed in a uniform way since the atoms have all the same mass. Two hybrid molecules or one hybrid and one AT molecule will interact partially via atom−atom interaction and partially via CG interaction on the COM, the amount of which is decided by the $w(x)$. As above, the force on the COM is then redistributed on the atoms.

dx.doi.org/10.1021/ct3003354 | J. Chem. Theory Comput. 2012, 8, 2878−2887

cannot define a Hamiltonian of the system. This aspect is discussed in the next section.

3. THERMODYNAMIC EQUILIBRIUM

The principle used in this case to build a conceptual framework to ensure equilibrium is the following: there must be a process of acquiring (releasing) some sort of thermodynamic information associated with acquiring (releasing) DOFs. An explicit example can clarify the idea; let us suppose that a molecule moves from the CG to the AT region. The molecule will be leaving a local environment of equilibrium; it will slowly acquire vibrational and rotational DOFs (as it acquires the AT resolution) and tries to enter in the AT region where other molecules are in local instantaneous equilibrium. At this point if the vibrational and rotational DOFs of the molecule are not compatible with those of the AT environment, it is likely that the molecule is sent back because it would perturb the local equilibrium in a massive way. In a similar way, thought less evident, a molecule going from the AT to the CG region should lose vibrational and rotational energy in order to properly accommodate with the CG environment (spheres). In this context the thermodynamic information consists of the free energy per DOFs (let us define it as $\phi(x)$) which the molecule needs to acquire (or remove) in order to equilibrate with the AT (CG) environment once it has changed resolution. In order to allow the process of molecular equilibration related to the transition from one region to another, three options have been explored so far. (i) The first is to employ a thermostat which acts locally and provides/removes this energy per DOFs. The accuracy of this approach is highly satisfactory from the numerical point of view (for example, the density in the most critical region, i.e., the transition region, has an accuracy of 5% wrt the target value). However, from the conceptual point of view this approach is not satisfactory since the amount of energy per DOFs is not distributed according to some controllable, physical principles, but it is distributed in a stochastic manner. A numerically as well as conceptually well founded approach is that based on the idea of thermodynamic force, that is, a force derived on the basis of thermodynamic relations. This idea gave rise to the following procedures. (ii) One can define $\phi(x) = \mu_{atom} - \mu(w(x))$; that is the difference between the chemical potential (effectively a free energy per particle) which characterizes the AT resolution and the chemical potential corresponding to the resolution defined by $w(x)$. In a previous work[11] it has been shown that this quantity can be calculated and the thermodynamic force, defined as the gradient of $\phi(x)$, applied to the COM of the molecule (in addition to the coupling force of eq 1). The accuracy regarding the particle density is higher than that obtained with approach i. However, the calculation of $\mu(w(x))$ is rather demanding, and thus ii, though conceptually better founded, would be computationally not efficient. Finally a new approach, here referred as iii, has been proposed, based on the idea of the adaptive scheme as an open system MD in an effective grand canonical framework.[12] The description of the latter approach is given in the next section; the current work proposes an extension of the computational procedure employed in procedure iii.

4. EFFECTIVE GRAND CANONICAL APPROACH

The starting point on which this idea is based is the coarse-grained procedure we employ, that is, the iterative Boltzmann inversion (IBI). For a detailed description of the IBI, see ref 13; here, we report only the necessary aspects which are of interest in the development of the procedure of this paper. The IBI is a so-called "structure based" CG procedure; that is, it matches the RDF, $g(r)$, of the CG model to that of the reference full AT simulation. In this way by construction the isothermal compressibility of the AT and CG is the same: $\kappa_{AT} = \kappa_{CG}$ (up to a very high accuracy)[14] and as a consequence particle number fluctuations are the same. However, the pressure is different: $P_{AT} \neq P_{CG}$ (for a detailed description of the relation between the IBI procedure with $g(r)$, κ, the particle number fluctuation and pressure see, e.g., ref 14). At this point there are two possible strategies: (a) add a pressure correction within the IBI procedure at the price of a less accurate match of the $g(r)$ (and thus $\rightarrow \kappa_{AT} \neq \kappa_{CG}$, and in turn the number particle fluctuations are not preserved); (b) keep $\kappa_{AT} = \kappa_{CG}$, and deal with a CG model where $P_{AT} \neq P_{CG}$. In this case strategy b is more appropriate; in fact, in an adaptive framework it is crucial to keep the particle number fluctuations correct so that they are not arbitrarily suppressed. If instead they are suppressed, then there is no assurance that the properties obtained, above all for liquids and soft matter systems characterized by strong local density fluctuations, are not a product of numerical artifacts. Next, the approach to deal with different pressures is explained. In Figure 4 it is pictorially shown the adaptive resolution set up and the consequences of interfacing an AT and a CG model characterized by different pressures.

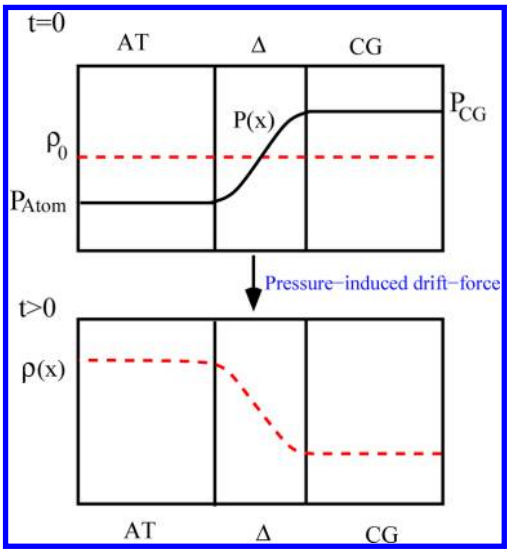

Figure 4. Adaptive resolution initial condition, for AT and CG with different pressure (top). As the simulation proceeds a pressure-induced force produces a drift of particle from the high pressure region to the low pressure region leading to an unphysical density profile.

As the simulation proceeds ($t > 0$) the initial condition of uniform density would not be kept because particles are pushed by the high pressure region to the low pressure region by a pressure-induced drift force. This, as a consequence, leads to a nonuniform, unphysical density profile. The solution to this problem is the derivation of a "thermodynamic force", that is, a force derived on the basis of thermodynamic principles, which compensates for the pressure-induced drift force. The thermodynamic principles employed here are the following; interfacing AT and CG models in terms of grand potential means: $P_{AT}V \neq P_{CG}V$; $\kappa_{AT} = \kappa_{CG}$; $\rho \neq \rho_0$. The reasons to write

dx.doi.org/10.1021/ct3003354 | J. Chem. Theory Comput. 2012, 8, 2878−2887

the thermodynamic relation in terms of grand potential are the following: (I) the grand potential is the natural thermodynamic potential when interfacing open systems, that is, systems which can exchange particles (the AT and CG are open to each other); (II) one can deal directly with the pressure (to which we have direct access) as a natural thermodynamic quantity to correct/adjust in order to obtain equilibrium. In this context a thermodynamic force $\mathbf{F}^{\mathrm{th}}(x)$ which restores equilibrium must be such that

$$\left[P_{\mathrm{AT}} + \frac{\rho_0}{M_\alpha}\int_\Delta \mathbf{F}^{\mathrm{th}}(x)\,\mathrm{d}x\right]V = P_{\mathrm{CG}}V;$$

$$\kappa_{\mathrm{AT}} = \kappa_{\mathrm{CG}} \text{ at } \rho = \rho_0 \tag{3}$$

The relation above expresses the situation of a subsystem (e.g.) AT, in equilibrium with a reservoir (e.g.) CG, despite $P_{\mathrm{AT}} \neq P_{\mathrm{CG}}$ and (most likely) $\mu_{\mathrm{AT}} \neq \mu_{\mathrm{CG}}$ (but with no need of specifying either μ_{AT} or μ_{CG}). In essence, the thermodynamic work generated or adsorbed by $\mathbf{F}^{\mathrm{th}}(x)$ removes the differences and ensures equilibrium. The explicit expression of $\mathbf{F}^{\mathrm{th}}(x)$ is

$$\mathbf{F}^{\mathrm{th}}(x) = \frac{M}{\rho_0}\nabla P(x) \tag{4}$$

That is, at $\rho = \rho_0$, eq 4 expresses the force on a molecule with mass M balancing the pressure-induced force, $-\nabla P(x)$. However $P(x)$ is not directly accessible from the simulation and would require a large number of additional runs which would make the procedure computationally not efficient (or as efficient as that of determining $\mu(x)$ in procedure ii). For this reason a linear approximation for $P(x)$ is used instead:

$$P(x) \approx P_{\mathrm{AT}} + \frac{M_\alpha}{\rho_0\kappa}[\rho_0 - \rho(x)] \tag{5}$$

where $\rho(x)$ is the density of particles generated by the pressure-induced drift-force. Next the thermodynamic force is obtained via an iterative (fastly converging) procedure, as

$$\mathbf{F}^{\mathrm{th}}_{k+1}(x) = \mathbf{F}^{\mathrm{th}}_{k}(x) - \frac{M_\alpha}{[\rho_0]^2\kappa}\nabla\rho_k(x) \tag{6}$$

with $\rho_k(x)$ density profile obtained by the application at the kth iteration of the $\mathbf{F}^{\mathrm{th}}_k(x)$. Therefore, for every iteration, an AdResS simulation is required to calculate the density profile. As a consequence, the adaptive coupling, in terms of force acting on the molecule, e.g., α is modified, from $\mathbf{F}_\alpha = \sum_\beta \mathbf{F}_{\alpha\beta}$ of eq 1 to

$$\mathbf{F}_\alpha = \sum_\beta \mathbf{F}_{\alpha\beta} + \mathbf{F}^{\mathrm{th}}(x_\alpha) \tag{7}$$

where x_α is the COM position of molecule α. The molecular force $\mathbf{F}_\alpha$ is further mapped onto each atom (if necessary) by the weight of the atomic mass over the molecular mass, namely, $\mathbf{F}_{\alpha_i} = (M_{\alpha_i})/(M_\alpha)\mathbf{F}_\alpha$, where $M_{\alpha i}$ is the mass of ith atom on molecule α. It is interesting to note that since $(\partial\mu/\partial\rho)_{V,T} = (1)/([\rho]^2\kappa)$, we can conclude that this procedure is conceptually equivalent to that labeled ii in the previous section, but with the advantage of a much higher computational efficiency. The approach outlined in this section has been named "effective grand canonical" because it has the characteristic of a standard grand canonical system regarding the coupling to a particle reservoir and because the particle number fluctuations in the AT e CG region are preserved. However, it is an "effective" approach because one does not have a direct access to the chemical potential μ (key quantity for a formal derivation of the partition function in the Grand Canonical ensemble) and because the particle reservoir is finite. The application to liquid water at ambient conditions[12] and to water−methanol mixtures[15] has proven that the method gives very accurate numerical results if compared with the (by far more expensive) full AT simulations of reference. This means that regarding the computational as well as conceptual robustness of the method the level reached is highly satisfying. However, in this work we attempt to define a path to a further systematic improvement, focusing on the reproduction of properties in the transition region Δ. This is reported in the next section.

5. SECOND ORDER CORRECTION TO THE COUPLING FORCE

The transition region Δ has a role of a filter that allows molecules to transit from one region to the other without perturbing the equilibrium of the AT and CG region. While properties in the AT and CG region have a physical meaning, Δ does not have any physical meaning but represents only a computationally convenient tool. In this sense, what is relevant is that quantities such as the $g(r)$, κ, and the local particle number fluctuations are the same in the AT and CG region (and in turn equal to those of a reference full AT simulation), but it is not necessary that they are the same in Δ. The only significant requirement in Δ is that the average particle density is the same as in AT and CG region; in fact depletion or increasing of density in Δ would create artifacts in the AT and CG region. The proper behavior of the density in Δ is assured by the application of $\mathbf{F}^{\mathrm{th}}(x)$. However, if there exists a systematic procedure which allows, without massive additional computational costs, also for the $g(r)$, κ, and the local particle number fluctuations to properly behave in Δ (that is to be as in the AT and CG region) and assures global thermodynamic equilibrium, then the coupling will be much smoother and would avoid the possibility of any artifacts at the boundaries of the various regions; moreover, by construction, the numerical accuracy should be higher also in the AT and CG region. In the following we show an approach which fulfills the requirements above. To do so, we extend the coupling formula, $\mathbf{F}_\alpha = \sum_\beta \mathbf{F}_{\alpha\beta} + \mathbf{F}^{\mathrm{th}}(x_\alpha)$, by adding a further force, which assures that the $g(r)$ in Δ is the same as in the AT and CG region, thus preserving κ and the particle number fluctuations without perturbing the thermodynamic equilibrium. We will refer to such an approach as "second order correction"; this is because while $\mathbf{F}^{\mathrm{th}}(x)$ is based on the correction of the first moment of the probability distribution of the system in phase space $\rho(x)$, the new additional term is derived as a correction to the second moment of the distribution, $g(r)$. The technical details of the procedure and the numerical results are shown in the next sections. Finally, we show that the correction to the $g(r)$ represents also a conceptual advancement; in fact, it implies that, at least at the level of the COM-COM $g(r)$ (for the conditional probability), the AT region is fully equivalent to a subsystem embedded in a larger full AT bath. This represents a natural step toward the grand canonical idea, and it gives more solid formal basis to the approach along this direction. To rigorously show that a subsystem in AdResS samples a grand canonical distribution, one should show that the joint distribution $p(\boldsymbol{x},N)$ (that is the probability of finding a certain configuration x for a given number of particles N) is the same

dx.doi.org/10.1021/ct3003354 | J. Chem. Theory Comput. 2012, 8, 2878−2887

as in a subsystem of a full atomistic simulation; this is the subject of future work.

6. DETERMINATION OF THE FORCE

The additional force which should be added up to the thermodynamic force in order to have a $g(r)$ in Δ as in the AT and CG region must satisfy the following requirements: (a) it should act only in Δ; (b) it should not perturb the properties of the AT and CG region and the overall equilibrium of the system. In order to fulfill the requirements above we have developed a scheme whose sequential steps are reported in the following.

(1) We proceed to the determination of $\mathbf{F}^{\mathrm{th}}(x)$ as reported in the previous section, according to the procedure of ref 12. This will ensure that we have the same ρ all over the simulation box, and to have the same $g(r)$ in the AT and CG region, but not in the transition region Δ.

(2) We correct the interpolation formula on the force by a force correcting the $g(r)$ in Δ:

$$\mathbf{F}_{\alpha\beta} = w_\alpha w_\beta \mathbf{F}^{\mathrm{AT}}_{\alpha\beta} + [1 - w_\alpha w_\beta]\mathbf{F}^{\mathrm{CG}}_{\alpha\beta} + w_\alpha w_\beta(1 - w_\alpha w_\beta)\mathbf{F}^{\mathrm{rdf}}_{\alpha\beta} \tag{8}$$

The $g(r)$ correction force $\mathbf{F}^{\mathrm{rdf}}$ is determined by the IBI scheme which in this case is

$$U^{\mathrm{rdf}}_{k+1}(r) = U^{\mathrm{rdf}}_{k}(r) + k_{\mathrm{B}}T \ln\left[\frac{g_k(r)}{g_{\mathrm{AT}}(r)}\right] \tag{9}$$

where $U^{\mathrm{rdf}}(r)$ is the pairwise correction potential applied to the molecule in Δ. The force is calculated by

$$\mathbf{F}^{\mathrm{rdf}}_{\alpha\beta} = \mathbf{F}^{\mathrm{rdf}}(\mathbf{r}_{\alpha\beta}) = -\nabla_r U(r_{\alpha\beta}) \tag{10}$$

The $g_{\mathrm{AT}}(r)$ is the target AT $g(r)$ that the hybrid region should reproduce, and $g_k(r)$ is the *average* hybrid RDF of the kth iteration. It must be noticed that the RDF correction force $\boldsymbol{F}^{\mathrm{rdf}}$ only depends on the relative position of two molecules, i.e., $\mathbf{r}_{\alpha\beta}$. Even though the $g(r)$ in Δ is actually a function of position x, here it is assumed that the RDF correction does not have this dependency. In the IBI scheme (eq 9), the RDF of the hybrid region at kth step $g_k(r)$ is averaged over the hybrid region, so that no spatial dependency exists in this iteration formula. The spatial dependency is added later by the prefactor $w_\alpha w_\beta(1 - w_\alpha w_\beta) = w(x_\alpha)w(x_\beta)[1 - w(x_\alpha)w(x_\beta)]$. The effectiveness of such an approach will be demonstrated in the next section. The initial guess of the potential is chosen as the potential of mean force

$$U^{\mathrm{rdf}}_0(r) = -k_{\mathrm{B}}T \ln g_{\mathrm{AT}}(r) \tag{11}$$

The prefactor $w_\alpha w_\beta(1 - w_\alpha w_\beta)$ is chosen such that the force acts only between molecules in Δ. In order to be sure that this is indeed the case we have also slightly modified the switching function $w(x)$ from the expression of eq 2 to the following:

$$w(x) = \begin{cases} 1 & x < d_{\mathrm{AT}} \\ 1 & d_{\mathrm{AT}} < x < d_{\mathrm{AT}} + r_c \\ \cos^2\left[\dfrac{\pi}{2(d_\Delta - r_c)}\right. & d_{\mathrm{AT}} + r_c \\ \left.(x - d_{\mathrm{AT}} - r_c)\right] & < x \\ & < d_{\mathrm{AT}} + d_\Delta \\ 0 & d_{\mathrm{AT}} + d_\Delta < x. \end{cases} \tag{12}$$

The definitions of d_{AT}, d_Δ, and x are the same as in eq 2, while r_c is the cutoff radius (which is the same for the Lennard-Jones interaction and the electrostatic interaction treated by the reaction field method); in this work, $d_\Delta \geq 2r_c$. In the water simulation presented in section 7, $d_{\mathrm{AT}} = 0.5$ nm, $d_\Delta = 2.75$ nm, and $r_c = 0.9$ nm. This new definition of $w(x)$ essentially consists of considering an extension (of size r_c) of the hybrid region to part of the AT region. In other words, the resolution of the molecules in the range $d_{\mathrm{AT}} < x < d_{\mathrm{AT}} + r_c$ are still atomistic ($w = 1$), but those molecules are considered as part of the system of the hybrid region Δ and not of the atomistic region. This assures that $\mathbf{F}^{\mathrm{rdf}}(\mathbf{r}_{\alpha\beta})$ acts only between molecules in the hybrid region, so that it does not perturb the interactions in the atomistic region. If not stated otherwise, the new weighting function eq 12 is applied to all AdResS forces.

(3) Applying the force obtained by the IBI will correct the $g(r)$ in the hybrid region; however, the density profile of the system will be disturbed. To fix this problem, we proceed by performing an additional iteration on the thermodynamic force (TFI) which corrects the density profile, followed by an IBI step to correct the possible perturbation of the $g(r)$ due to the previous iteration of the thermodynamic force. Therefore, the resulting scheme consists of an iterative Boltzmann inversion-thermodynamic force iteration correction loop (IBI-TFI correction loop) to reproduce the correct density profile and $g(r)$ in Δ at the same time, (see Algorithm 1).

In the next section we will show the application of the method to the case of liquid water at ambient condition as in ref 12. We will show that higher accuracy regarding the $g(r)$ and the particle number fluctuation in Δ can be reached and that basic thermodynamic relations (as the grand potential) are not perturbed by the additional correction on the forces.

7. APPLICATION TO LIQUID WATER

Figure 5 shows the AdResS set up for a system consisting of liquid water at ambient conditions (as in ref 12) to which we have applied the procedure reported in the previous section (technical details of the simulation can be found in the Appendix). Here we show the numerical results for liquid water and prove that our approach represents a successful refinement of the original method of ref 12. Figure 6 shows the $g(r)$ in the Δ region after the IBI-TFI iteration loop is applied. The agreement with the reference all atom calculation is highly satisfactory. Moreover, the comparison with the results obtained employing the thermodynamic force only (as in ref 12) shows that the additional force, $\mathbf{F}^{\mathrm{rdf}}$, proposed here allows for a sizable improvement of the structural consistency across the simulation box. The accuracy reached in this case becomes more evident if one considers the $g(r)$ calculated locally in subregions of Δ across the box; this is shown in Figure 7. In the situation where the disagreement on the $g(r)$ in Δ between the AdResS of ref 12 and the reference all atom simulation is larger,

Algorithm 1 IBI-TFI correction loop

Require: $\mathbf{F}_0^{\mathrm{th}}$ and $\mathbf{F}_0^{\mathrm{rdf}}$
$\mathbf{F}^{\mathrm{th}} \leftarrow \mathbf{F}_0^{\mathrm{th}}$, $\mathbf{F}^{\mathrm{rdf}} \leftarrow \mathbf{F}_0^{\mathrm{rdf}}$
repeat
  $\mathbf{F}_1^{\mathrm{rdf}} \leftarrow \mathbf{F}^{\mathrm{rdf}}$
  for $k = 1$ to N_{IBI} **do**
    AdResS simulation using $\mathbf{F}^{\mathrm{th}}$ and $\mathbf{F}_k^{\mathrm{rdf}}$
    calculate hybrid RDF $g_k(r)$
    $U_{k+1}^{\mathrm{rdf}}(r) \leftarrow U_k^{\mathrm{rdf}}(r) + k_B T \ln\left[\frac{g_k(r)}{g_{\mathrm{AT}}(r)}\right]$
    $\mathbf{F}_{k+1}^{\mathrm{rdf}}(\mathbf{r}) \leftarrow -\nabla_{\mathbf{r}} U_{k+1}^{\mathrm{rdf}}(r)$
  end for
  $\mathbf{F}^{\mathrm{rdf}} \leftarrow \mathbf{F}_{N_{\mathrm{IBI}}+1}^{\mathrm{rdf}}$
  $\mathbf{F}_1^{\mathrm{th}} \leftarrow \mathbf{F}^{\mathrm{th}}$
  for $k = 1$ to N_{TFI} **do**
    AdResS simulation using $\mathbf{F}_k^{\mathrm{th}}$ and $\mathbf{F}^{\mathrm{rdf}}$
    calculate density $\rho_k(x)$
    $\mathbf{F}_{k+1}^{\mathrm{th}}(x) \leftarrow \mathbf{F}_k^{\mathrm{th}}(x) - \frac{M}{\rho_0^2 \kappa_T} \nabla \rho_k(x)$
  end for
  $\mathbf{F}^{\mathrm{th}} \leftarrow \mathbf{F}_{N_{\mathrm{TFI}}+1}^{\mathrm{th}}$
until both $\mathbf{F}^{\mathrm{th}}$ and $\mathbf{F}^{\mathrm{rdf}}$ are converged

$\mathbf{F}_0^{\mathrm{th}}$ is determined following the procedure of Ref.,[12] the initial guess, $\mathbf{F}_0^{\mathrm{rdf}}$ is the potential of mean force. The structure of the Algorithm 1 is rather simple though efficient: in the outermost loop, the IBI and TFI are executed consequently, with fixed number of iterations N_{IBI} and N_{TFI}, respectively. In practice, the TFI converges faster than IBI, so $N_{\mathrm{TFI}} = 2$ and $N_{\mathrm{IBI}} = 50$ provides results with satisfying accuracy.

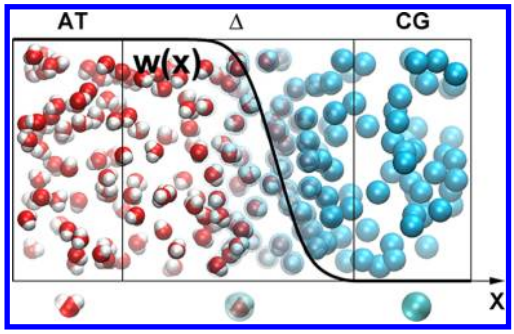

Figure 5. Schematic representation of the adaptive simulation box for water where the new proposed $w(x)$ is plotted. Essentially, the Δ region includes a part with full AT resolution. This makes sure that $\mathbf{F}^{\mathrm{rdf}}(r_{\alpha\beta})$ acts only between molecules which are interacting via hybrid resolution. The new form of $w(x)$ does not have any further consequence on the system. The Δ region considered here is, for technical reasons, larger than the AT and CG region; in fact, a Δ region, larger than the AT and CG region, for the adaptive process is a "worst case scenario". This must be intended in the sense that if the approach proposed here works well with a small AT and CG region (for which a relatively larger Δ region is a strong perturbation), then it will work well the case where such two regions AT and CG are much larger than Δ.

that is the central region of Δ (of about 9.0 nm extension, bottom-left panel in Figure.7), the application of the IBI-TFI correction loop instead significantly improves the situation. Next we must show that the IBI-TFI correction loop does not perturb the uniform density profile across the box. Figure 8 shows that, at the very first step of the procedure, when $\mathbf{F}^{\mathrm{rdf}}(\mathbf{r}_{\alpha\beta})$ is applied and $\mathbf{F}^{\mathrm{th}}$ is not updated, the density is perturbed. However, despite this initial perturbation, already at the first step of the IBI-TFI iteration loop the density converges toward a uniform profile and only four steps are required to

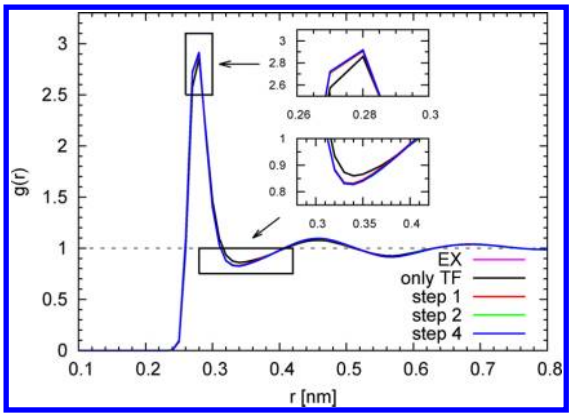

Figure 6. $g(r)$ in Δ after the IBI-TFI correction loop is applied. The curves obtained after the first, second, and fourth iteration step are represented in red, green, and blue solid lines, respectively. The curve obtained from the reference explicit all atom calculation (EX) is represented with a solid pink line. However, it must be noted that this latter is overlapping with the other lines, and cannot be seen from the plot. The curve obtained by applying simply the thermodynamic force correction (only TF), thus without correction on the $g(r)$, is in black. The two insets show the details at the first peak and the first valley. As can be seen, after only four iterations $\mathbf{F}^{\mathrm{rdf}}(\mathbf{r}_{\alpha\beta})$ allows the reproduction, in Δ, with high accuracy the $g(r)$ of the reference full AT calculation.

have a highly satisfied agreement with the results of the explicit all atom reference simulation. The fast convergence of the iteration loop is also shown in terms of the convergence of the potential correcting the RDF in Figure 9. More important, the inset shows the convergence of work done by $\mathbf{F}^{\mathrm{th}}$: $\int_\Delta \mathbf{F}^{\mathrm{th}}\, dx$, as a function of the number of iteration steps. This is important information because it tells us that the presence in the iterative loop of $\mathbf{F}^{\mathrm{rdf}}(\mathbf{r}_{\alpha\beta})$ does not perturb the role of the resulting $\mathbf{F}^{\mathrm{th}}$ in fulfilling the thermodynamic relation of eq 3 and thus in providing the thermodynamic equilibrium. The difference now is that also the structural transition occurs in a much smoother way. A sizable effect of this smoother transition is shown in Figure 10 where the molecular particle number fluctuation is plotted as a function of the position in Δ. While the results of the original method of ref 12 show an evident deviation from the results of the reference all atom simulation, for the case where the TFI-IBI loop is applied there is a satisfactory agreement and basically the two curves overlap within the error bar. This assures that particle number fluctuations are the same as in the AT and CG region and that no artifact due to wrong fluctuation properties can propagate into the AT and CG region. It must be noticed that the accurate reproduction of the particle number fluctuation also suggests that the compressibility in the Δ region is accurately reproduced. However, there is a subtle difference between these two concepts: they are related to each other via an equation, only in the thermodynamic limit, which is not the case of the small finite system of Δ. This implies that we could perhaps argue that the compressibility in Δ may not go particularly wrong; however, we cannot make any precise statement regarding its accuracy.

8. THEORETICAL CONSIDERATIONS

Let us consider the dynamics of a system that is subject to the Langevin equation (that is the thermostat usually employed in the AdResS simulations):

$$d\mathbf{r}_i = \mathbf{v}_i\, dt \tag{13}$$

dx.doi.org/10.1021/ct3003354 | J. Chem. Theory Comput. 2012, 8, 2878−2887

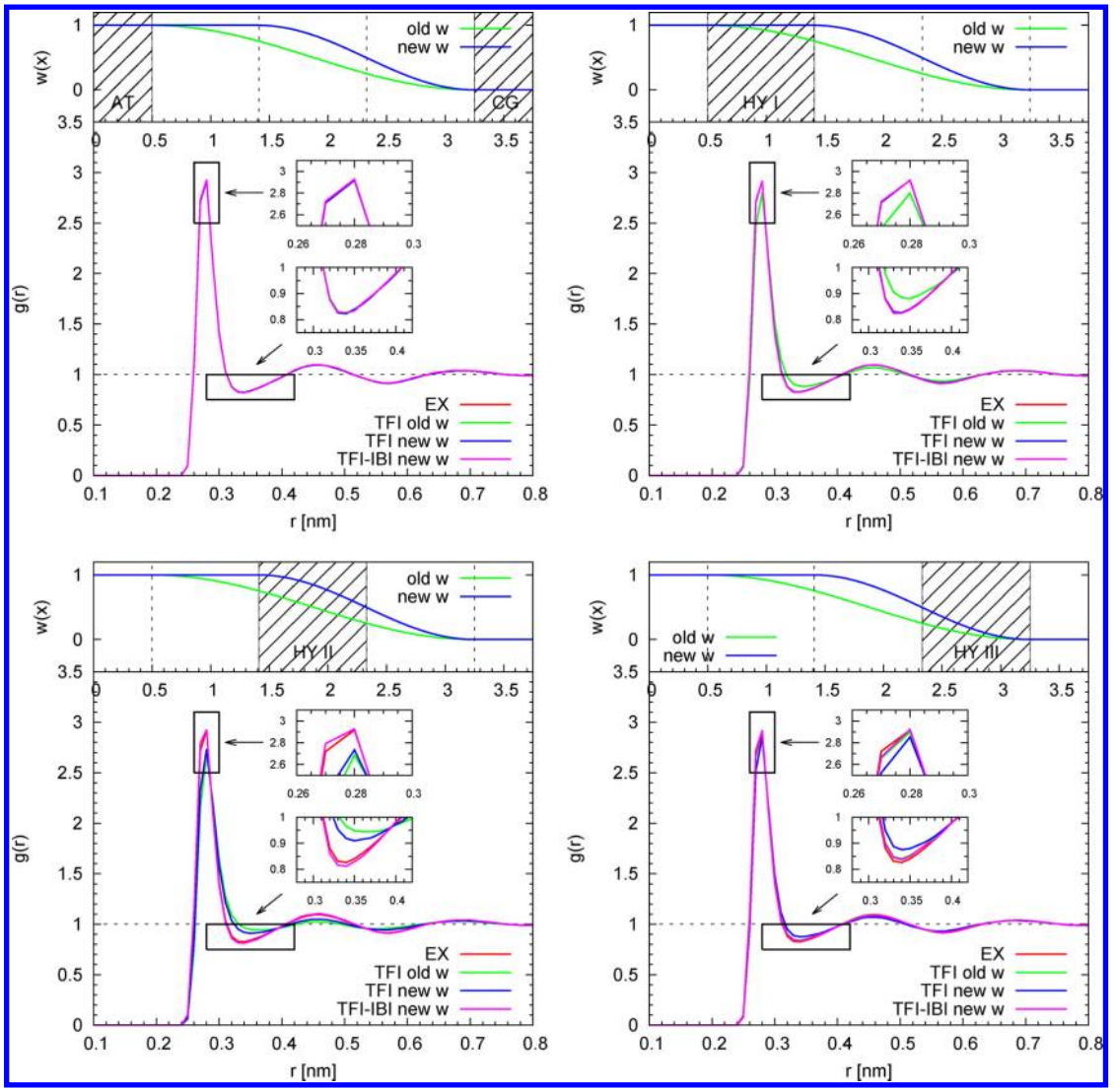

Figure 7. Local $g(r)$'s. The red line is the curve corresponding to the reference explicit (all atom) simulation (EX). The curves corresponding to the simulation where only the thermodynamic force is applied, for the case of the old weighting function eq 2 and the new weighting function eq 12, are denoted by the green and blue lines, respectively. The curve obtained by employing the TFI-IBI method is represented in pink. The hybrid region is equally divided into three parts, HY I, HY II, and HY III, the widths of which are roughly equal to the cutoff radius, i.e., 9 nm. The top part of each panel shows the region where the $g(r)$ is calculated. The top left panel corresponds to the AT and CG case, the top right to the subregion HY I of Δ, closer to the AT region; the bottom left panel corresponds to the subregion HY II of Δ, where the level of hybridicity is the highest, and thus the most delicate case. The bottom-right panel corresponds to the subregion HY III of Δ, that is closer to the CG region. The insets show the details at the first peak and the first valley.

$$m_i\, \mathrm{d}\mathbf{v}_i = [-m_i\xi_i\mathbf{v}_i + \mathbf{F}_i]\mathrm{d}t + \sqrt{2\sigma_i}\, \mathrm{d}\mathbf{W}_t \tag{14}$$

Here $\mathrm{d}\mathbf{W}_t$ is the standard Wiener process. If the system has a potential, namely $\mathbf{F}_i = -\nabla_{r_i}U$, then it can be proven that the Langevin dynamics generates the canonical ensemble

$$p(\mathbf{r}_1, \cdots, \mathbf{r}_N, \mathbf{v}_1, \cdots, \mathbf{v}_N) \propto \exp[-\beta\mathcal{H}(\mathbf{r}_1, \cdots, \mathbf{r}_N, \mathbf{v}_1, \cdots, \mathbf{v}_N)] \tag{15}$$

where $\mathcal{H}$ is the Hamiltonian of the system:

$$\mathcal{H}(\mathbf{r}_1, \cdots, \mathbf{r}_N, \mathbf{v}_1, \cdots, \mathbf{v}_N) = \sum_{i=1}^{N} \frac{1}{2} m_i \mathbf{v}_i^2 + U(\mathbf{r}_1, \cdots, \mathbf{r}_N) \tag{16}$$

Let us first consider the case where we have N_1 molecules in the atomistic region, N_2−N_1 molecules in the hybrid region. Without loss of generality, we assume molecules 1, ..., N_1 are in the atomistic region, molecules N_1 + 1, ..., N_2 are in the hybrid region, and N_2 + 1, ..., N are in the coarse-grained region. The pair $\{r_i, v_i\}$ of the atomistic representation denotes the COM position and velocity of the ith molecule. For convenience, we only consider the COM coordinates of the AT molecule; all the arguments employed here can be easily extended to treat each atom of the molecule. We hereby consider the AT region as a subsystem of the whole system, which is composed by the AT, Δ, and CG regions. We must always keep in mind that our reference system is the full AT case. Thus, the properties of the AT subsystem in AdResS must be the same for the equivalent subsystem in a full AT case. If we (hypothetically) fix the coordinates of the molecules in Δ, according to the definition of $w(x)$ in eq 12, the Hamiltonian in the AT region can be written as

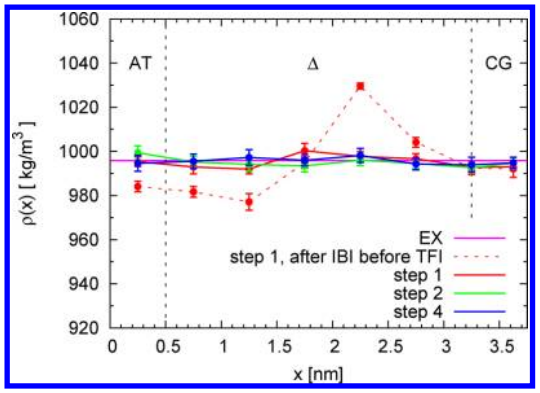

Figure 8. Particle density across the simulation box. The reference data from the all atom simulation (EX) are reported in pink. The red broken line corresponds to the situation after the correction on the $g(r)$ is applied, but the thermodynamic force is not yet updated. The solid red, green, and blue lines represent steps 1, 2, and 4 of the IBI-TFI loop. The agreement with the reference data is highly satisfactory.

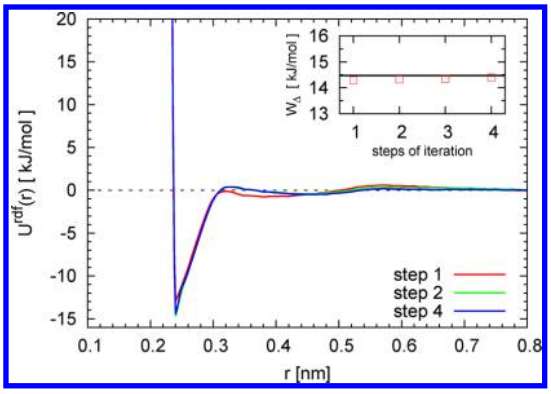

Figure 9. Plot shows the potential obtained by the IBI iteration to correct the $g(r)$ in Δ; the convergence is shown to be rather fast. The inset shows the convergence toward the target value of the integral $\int_{\Delta}\mathbf{F}^{\mathrm{th}}\,dx$ (i.e., the value obtained without correcting the $g(r)$ in Δ) as a function of the IBI-TFI iteration steps. This is an important result; in fact, this quantity represents the work adsorbed or produced in order to have thermodynamic equilibrium in the system. The result shows that the correction force for the $g(r)$ in Δ does not perturb the overall thermodynamic relation of equilibrium.

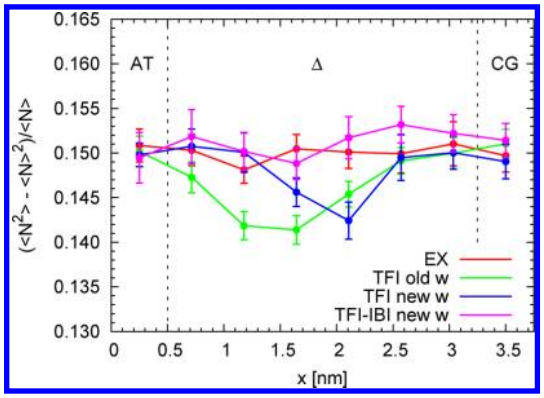

Figure 10. Particle number fluctuation in Δ. The reference data from a full atomistic simulation are reported in red (EX). The green line represents results obtained with the original formulation, blue with the new $w(x)$ but without the application of the TFI-IBI loop, and pink the results of the new method.

$$\mathcal{H}^{\mathrm{AT}}(\mathbf{x}_1;\,\mathbf{x}_2) = \sum_{j=1}^{N_1}\frac{1}{2}m_i\mathbf{v}_i^2 + \sum_{i,j=1}^{N_1}\frac{1}{2}U^{\mathrm{AT}}(\mathbf{r}_i - \mathbf{r}_j) + \sum_{i=1}^{N_1}\sum_{j=N_1+1}^{N_2}U^{\mathrm{AT}}(\mathbf{r}_i - \mathbf{r}_j) \tag{17}$$

Here we denote the phase space variables: $\mathbf{x}_1 = (\mathbf{r}_1,..., \mathbf{r}_{N_1}, \boldsymbol{\nu}_1,..., \boldsymbol{\nu}_{N_1})$, $\mathbf{x}_2 = (\mathbf{r}_{N_1+1},..., \mathbf{r}_{N_2}, \boldsymbol{\nu}_{N_1+1},..., \boldsymbol{\nu}_{N_2})$, and $\mathbf{x}_3 = (\mathbf{r}_{N_2+1},..., \mathbf{r}_N, \boldsymbol{\nu}_{N_2+1},..., \boldsymbol{\nu}_N)$. $\mathbf{x}_3$ denotes the coordinates and velocities of the COM of the molecules in the CG region and for the moment do not enter in our derivation. It must be noticed that the writing of the formula 17 above is possible because the long-range electrostatic interaction is treated by the reaction field method; therefore, there is indeed no long-range interaction in the system. This means that molecules in the AT region are interacting only with those in the hybrid region, with the cutoff radius r_c. Second, by the new definition of $w(x)$, i.e. eq 12, the molecules in the AT region interact with the molecules in the hybrid in an atomistic fashion, because every hybrid molecule falling within the cutoff of an atomistic molecule actually has a weighting function of $w = 1$, which means their nature is atomistic though we treat them as hybrid. Here we can consider $\mathbf{x}_1$ to be the variable and $\mathbf{x}_2$ a certain (fixed) external molecular environment. According to the Langevin dynamics, we have the conditional probability distribution:

$$p(\mathbf{x}_1|\mathbf{x}_2) \propto \mathrm{e}^{-\beta\mathcal{H}^{\mathrm{AT}}(\mathbf{x}_1;\mathbf{x}_2)} \tag{18}$$

Here under the hypothesis of fixed number of particles (however the argument applies for any combination of N_1, N_2), we want to derive a minimal consistency criterion for the conditional probability; that is, under which conditions this probability is the same as that of the equivalent region in a full atomistic system of reference. We will show that matching the $g(r)$ also in the **Δ** region assures at basic level such a consistency, and thus, it shows the importance of the criterion based on the $g(r)$ which we have developed in this paper. Accordingly, the phase space distribution of the AT region writes

$$p(\mathbf{x}_1) = \int p(\mathbf{x}_1|\mathbf{x}_2)\cdot p(\mathbf{x}_2)\,d\mathbf{x}_2 \tag{19}$$

If the distribution $p(\mathbf{x}_2)$ is equivalent to that of the corresponding region in a full AT reference system, then one can consider the AT region in AdResS to be the equivalent of a subsystem embedded in a very large AT system. The crucial question is if $p(\mathbf{x}_2)$ is equivalent to that of a full AT system. Most likely this is not the case, at least for the interpolation scheme plus the thermodynamic force. In fact if one considers $p(\mathbf{x}_2)$ expanded in terms of its momenta, by performing simulations using the coupling scheme of eq 7, the first order of $p(\mathbf{x}_2)$ is correct (i.e., the particle density), but already at the second order, that is the COM-COM RDF, the hybrid region deviates from the other two regions. However, as we have shown in the previous sections, one can add a further corrective force in the hybrid region and obtain a RDF as that of the AT and CG region. This would mean that the idea of the AT region as a subsystem of a very large AT system, at least at the basic level corresponding to the hypothesis done here, is correct up to the second order in terms of distribution. This we have shown is more than sufficient for numerical accuracy.

dx.doi.org/10.1021/ct3003354 | J. Chem. Theory Comput. 2012, 8, 2878−2887

9. CONCLUSIONS

We have proposed an extension of the effective grand canonical formulation of the adaptive resolution method. In the adaptive approach, it is important that structural properties and basic thermodynamic quantities in the AT and CG region are the same as in the reference full AT simulation, while the transition region Δ has no physical meaning and represents only a computational tool to favor the change of resolution keeping the overall equilibrium of the system. In the original formulation of the effective grand canonical AdResS, only the particle density in Δ is assured to be the same as in the AT and CG region. This requirement is crucial since depletion or excess of particles in Δ implies a higher/lower density in the AT and CG region and thus a situation different from the reference full AT system. However if one constructs a systematic procedure which preserves the thermodynamic equilibrium (as in the current formulation) but goes beyond the requirement of density in Δ and assures that further structural (radial distribution function) as well as thermodynamic properties (isothermal compressibility and the related particle number fluctuations) are reproduced in this region, then the transition from AT to coarse-grained resolution (and vice versa) would be even smoother and avoid any possible artifact at the border of the AT and CG region. In this work we have proposed such a procedure. It is based on a loop consisting of correcting the $g(r)$ in Δ and refining the thermodynamic force for the overall thermodynamic equilibrium. Though computationally more demanding than the original formulation (due to this additional loop), it shows that the smoothness of the transition from one resolution to the other can be systematically improved. While for adaptive resolution simulations of liquid water the accuracy of the original formulation is already highly satisfactory, there may exist systems where the importance of the particle number fluctuations in Δ can play a central role for a smooth transition. This is the case of larger molecules or polymers[16] and certainly for the quantum/path integral version of the adaptive method,[17−19] since this latter is based on the ring-polymer representation of atoms and molecules. Moreover we have given theoretical arguments that show how the agreement on the $g(r)$ in Δ justifies, up to the second order, the view of the AT system in AdResS as an equivalent subsystem in a large full AT system and thus gives more solid arguments toward the interpretation of the AT region as an effective Grand Canonical ensemble.

10. APPENDIX

The testing system contained 3456 SPC/E[20] water molecules in a 7.50 nm ×3.72 nm ×3.72 nm periodic box. The system was divided along the x direction into one atomistic region of width 1.00 nm and one coarse-grained region of width 1.00 nm connected by two hybrid region of width 2.75 nm. The simulation was made at room temperature of 300 K. The time step was Δt = 0.002 ps. The cutoff radius r_c used for all interactions was 0.90 nm. The electrostatic interaction method used for the atomistic region was the reaction field method. All simulations were performed by MD simulation software Gromacs[21] and VOTCA.[22]

AUTHOR INFORMATION

Corresponding Author

*E-mail: luigi.dellesite@fu-berlin.de.

Notes

The authors declare no competing financial interest.

ACKNOWLEDGMENTS

We thank Sebastian Fritsch for the help in guiding us in the use of the AdResS code at the initial stage of the project.

This work was partially supported by the Deutsche Forschungsgemeinschaft (DFG) with the Heisenberg grant provided to L.D.S (grant code DE 1140/5-1) and by ITN Nanopoly provided to H.W and C.S.

REFERENCES

(1) Praprotnik, M.; Delle Site, L.; Kremer, K. Multiscale simulation of soft matter: From scale bridging to adaptive resolution. *Annu. Rev. Phys. Chem.* **2008**, *59*, 545−571.

(2) Praprotnik, M.; Delle Site, L.; Kremer, K. Adaptive resolution molecular-dynamics simulation: Changing the degrees of freedom on the fly. *J. Chem. Phys.* **2005**, *123*, 224106.

(3) Praprotnik, M.; Delle Site, L.; Kremer, K. Adaptive resolution scheme for efficient hybrid atomistic-mesoscale molecular dynamics simulations of dense liquids. *Phys. Rev. E* **2006**, *73*, 066701.

(4) Ensing, B.; Nielsen, S. O.; Moore, P. B.; Klein, M. L.; Parrinello, M. Energy conservation in adaptive hybrid atomistic/coarse-grain molecular dynamics. *J. Chem. Theory Comput.* **2007**, *3*, 1100.

(5) Heyden, A.; Truhlar, D. G. Conservative algorithm for an adaptive change of resolution in mixed atomistic/coarse-grained multiscale simulations. *J. Chem. Theory Comput.* **2008**, *4*, 217.

(6) Shi, Q.; Izvekov, S.; Voth, G. A. Mixed atomistic and corase-grained molecular dynamics: Simulation of a membrane-bound ion channel. *J. Phys. Chem. B* **2006**, *110*, 15045.

(7) Izvekov, S.; Voth, G. A. Mixed resolution modeling of interactions in condensed phase systems. *J. Chem. Theory Comput.* **2009**, *5*, 3232.

(8) Nielsen, S. O.; Moore, P. B.; Ensing, B. Adaptive multiscale molecular dynamics of macromolecular fluids. *Phys. Rev. Lett.* **2010**, *105*, 237802.

(9) Praprotnik, M.; Poblete, S.; Delle Site, L.; Kremer, K. Comment on adaptive multiscale molecular dynamics of macromolecular fluids. *Phys. Rev. Lett.* **2011**, *107*, 99801.

(10) Delle Site, L. Some fundamental problems for an energy-conserving adaptive-resolution molecular dynamics scheme. *Phys. Rev. E* **2007**, *76*, 047701.

(11) Poblete, S.; Praprotnik, M.; Kremer, K.; Delle Site, L. Coupling different levels of resolution in molecular simulations. *J. Chem. Phys.* **2010**, *132*, 114101.

(12) Fritsch, S.; Poblete, S.; Junghans, C.; Ciccotti, G.; Delle Site, L.; Kremer, K. Adaptive resolution molecular dynamics simulation through coupling to an internal particle reservoir. *Phys. Rev. Lett.* **2012**, *108*, 170602.

(13) Reith, D.; Pütz, M.; Müller-Plathe, F. Deriving effective mesoscale potentials from atomistic simulations. *J. Comput. Chem.* **2003**, *24*, 1624−1636.

(14) Wang, H.; Junghans, C.; Kremer, K. Comparative atomistic and coarse-grained study of water: What do we lose by coarse-graining? *Eur. Phys. J. E: Soft Matter Biol. Phys.* **2009**, *28*, 221−229.

(15) Mukherji, D.; van der Vegt, N. F. A.; Kremer, K.; Delle Site, L. Kirkwood-buff analysis of liquid mixtures in an open boundary simulation. *J. Chem. Theory Comput.* **2012**, *8*, 375−379.

(16) Praprotnik, M.; Poblete, S.; Kremer, K. Statistical physics problems in adaptive resolution computer simulations of complex fluids. *J. Stat. Phys.* **2011**, *145*, 946−966.

(17) Poma, A. B.; Delle Site, L. Classical to path-integral adaptive resolution in molecular simulation: Towards a smooth quantum-classical coupling. *Phys. Rev. Lett.* **2010**, *104*, 250201.

(18) Poma, A. B.; Delle Site, L. Adaptive resolution simulation of liquid para-hydrogen: Testing the robustness of the quantum-classical adaptive coupling. *Phys. Chem. Chem. Phys.* **2011**, *13*, 10510−10519.

(19) Potestio, R.; Delle Site, L. Quantum locality and equilibrium properties in low-temperature parahydrogen: A multiscale simulation study. *J. Chem. Phys.* **2012**, *136*, 54101.
(20) Berendsen, H. J. C.; Grigera, J. R.; Straatsma, T. P. The missing term in effective pair potentials. *J. Phys. Chem.* **1987**, *91*, 6269−6271.
(21) Hess, B.; Kutzner, C.; van der Spoel, D.; Lindahl, E. Gromacs 4: Algorithms for highly efficient, load-balanced, and scalable molecular simulation. *J. Chem. Theory Comput.* **2008**, *4*, 435−447.
(22) Rühle, V.; Junghans, C.; Lukyanov, A.; Kremer, K.; Andrienko, D. Versatile object-oriented toolkit for coarse-graining applications. *J. Chem. Theory Comput.* **2009**, *5*, 3211−3223.